THE DESIGN AND CONSTRUCTION OF APPARATUS FOR PROBE MEASUREMENTS IN GASES

by

EUGENE ROY ASTLEY

A THESIS

submitted to

OREGON STATE COLLEGE

in partial fulfillment of
the requirements for the
degree of

MASTER OF SCIENCE

June 1950

APPROVED:

[redacted]

Professor of Physics

In Charge of Major

[redacted]

Head of Physics Department

[redacted]

Chairman of School Graduate Committee

[redacted]

Dean of Graduate School

Date thesis is presented May 12, 1950

Typed by Betty Davis

TABLE OF CONTENTS

I Theory of the Glow Discharge

A. Qualitative Discussion

1. Cathode Glow 2
2. Crookes Dark Space 3
3. Negative Glow 3-4
4. Faraday Dark Space 5
5. Positive Column 5-7

B. Quantitative Discussion

1. Electron Temperature 9
2. Electron Current Density 10
3. Electron Density 10
4. Positive Ion Temperature 10

II Construction of the Apparatus

A. Slotting of the Tube 11-12

B. Tube Variables 13-15

C. Construction 18-20

III Circuit Diagram 21

IV Experimental Results 22-24

THE DESIGN AND CONSTRUCTION OF APPARATUS FOR PROBE MEASUREMENTS IN GASES

Theory of the Glow Discharge

The Langmuir probe method of studying gaseous discharges has proved to be a valuable tool. In spite of this, its use has not been as widespread as might be expected. The tube described in this thesis has been designed primarily for student use in the laboratory. Its special feature is the use of a probe which can be moved by means of an external magnet while not disturbing the discharge. Before describing the tube which was built and tested, a theory of the probe will be given.

Theoretically, it should be possible to derive an equation to describe completely the phenomena occurring in glow discharges. Unfortunately, no completely satisfactory equation has been developed. Sir J. J. Thomson has attacked the problem taking into account such effects as ionization, recombination, mobility, diffusion and space-charge. (9, pp. 292-469) He has obtained solutions of the equations only for a few restricted cases. Before developing the mathematical formulas involved, it would seem pertinent to discuss the subject qualitatively.

Let us suppose that we have a tube filled with air at an appropriate pressure, the tube being long in comparison to its diameter, enclosing two plane-parallel electrodes. Apply then an adequate d.c. source such that a striated glow discharge is evident. The conditions necessary for the glow discharge are a sufficient applied potential difference and a gas at any pressure not so low as to give too infrequent collisions nor so high as to cause electrons to reach their terminal speeds at values below that necessary for ionization. (2, p. 333)

The discharge is a "steady-state self-sustaining discharge" (8, p. 568) in that the secondary electrons liberated from the cathode by positive ion bombardment produce, in ionization by collision, enough new electrons to maintain the current through the tube at its constant value.

One very striking feature of the glow discharge is the appearance of light and dark regions throughout the tube as may be seen in the photograph on the following page. Starting at the cathode in order of appearance they are: cathode glow, Crookes dark space, negative glow, Faraday dark space and the positive column. Each of these regions will be discussed separately in the following material.

The secondary electrons emitted from the cathode by positive ion bombardment usually have low energies and before they receive additional energy from the field, they form a small negative space-charge cloud close to the cathode; however, this does not seem to be the cause of the orange cathode glow occurring at the cathode surface. One might expect the maximum light intensity from the excitation

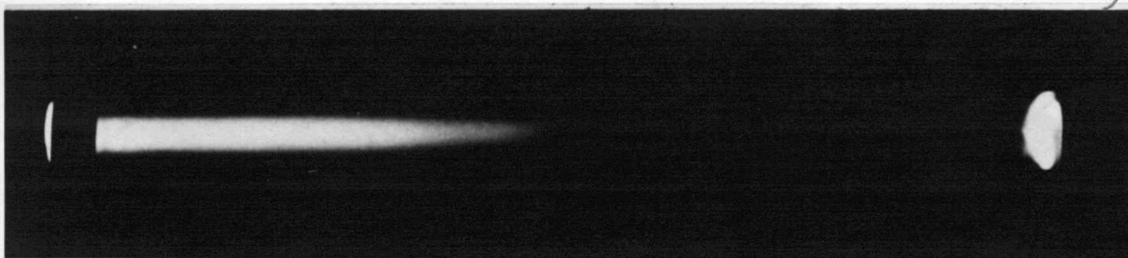

Pressure 3 mm Potential 1.5 kv

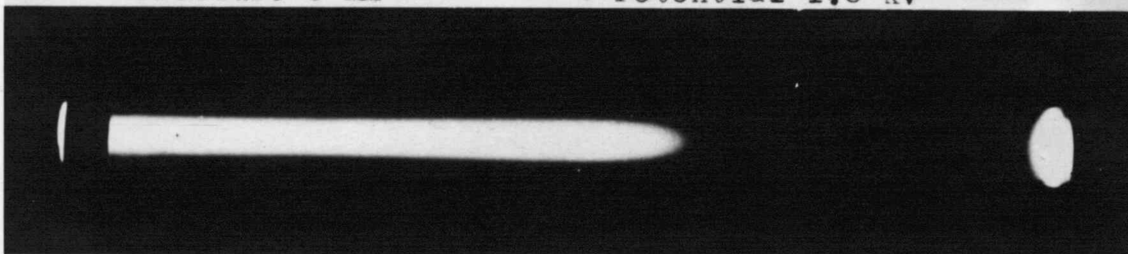

Pressure 1.5 mm Potential 1.5 kv

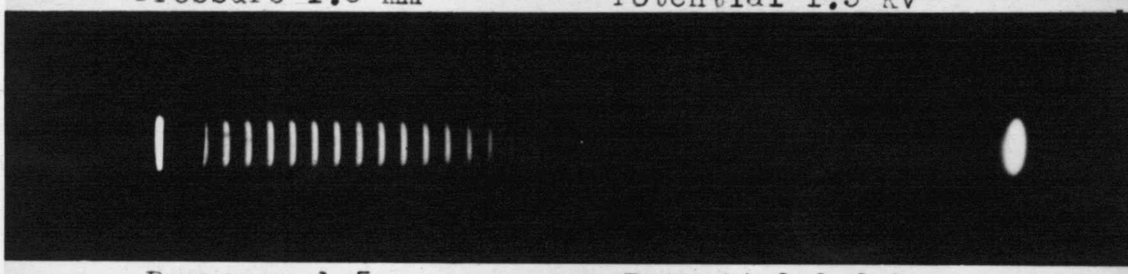

Pressure 1.5 mm Potential 1.0 kv

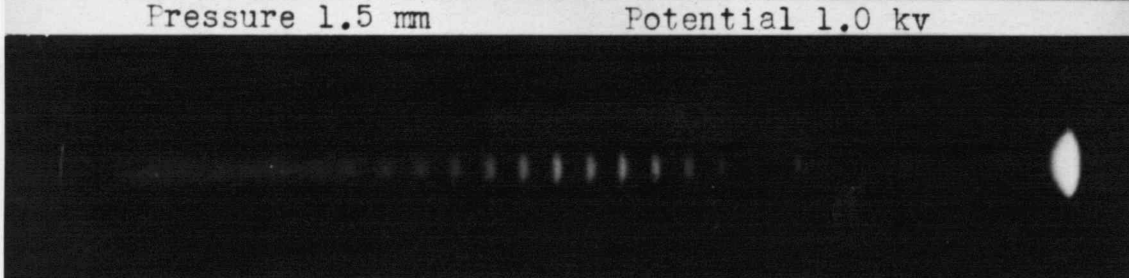

Pressure 500 microns Potential 1.0 kv

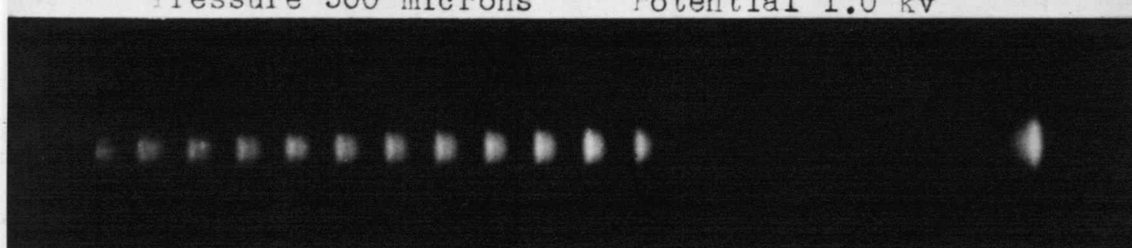

Pressure 200 microns Potential 1.0 kv

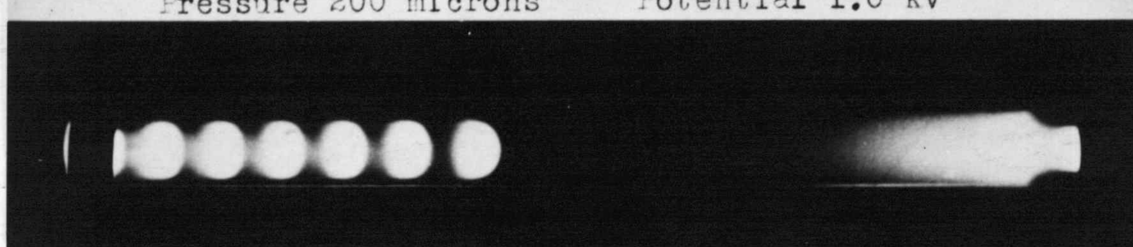

Pressure 30 microns Potential 1.3 kv

due to secondary electrons to occur close to the cathode, but spectroscopy experiments show this not to be the case. It would seem, however, that the cathode glow results from excitation by positive ions (5, p. 143) or fast ions originating from charge transfer at the cathode.

At low currents the cathode glow does not cover the entire electrode surface as the current goes only to a part of the cathode, the surface of the covered part being proportional to the current. This discharge is designated as the "normal" discharge with a "normal" cathode fall of potential. The normal cathode fall is nearly independent of the current and the pressure. If the current is increased above the value where the whole cathode is covered by the glow, the cathode fall will increase and we obtain an "abnormal" discharge. Discharges in certain gases actually have a glow composed of three different forms of light layers, of which only the center layer is the cathode glow caused by recombination. The other two are excitation of molecules by secondary electrons and light from sputtering.

Knowledge of the electric field, the ion and electron currents, and energies in the Crookes dark space for normal glow is very meager today due to the fact that the method of cold probe measurements devised by Langmuir and Mott-Smith (7, pp. 449, 538, 616, 762, 810) fails in regions of high field strength and non-Maxwellian velocity distributions. The field strength in this region seems to be largest near the cathode and decreases monotonously to the negative glow where the field strength is small. The length of the Crookes dark space usually is four to seven times the electron mean free path. In the normal discharge, many of the positive ions reaching the cathode are formed in the Crookes dark space, the rest being supplied from the negative glow. Also there is a speeding up of the secondary electrons from the cathode in the dark space and these enter the negative glow with high energies. Electrons exist in this stream with energies up to eighty per cent of the cathode fall. These fast electrons leave behind a region of positive space charge, the mobility of the positive ions being much less than that of the electrons. Recombination is infrequent because of the strong fields and high speed of the electrons. It should be realized that the Crookes dark space is not really dark but just represents a region of relatively little excitation and ionization.

The negative glow is the bluish luminous discharge which starts at the end of the dark space. The brightness of the glow diminishes as we recede from the cathode and the position of its end depends upon the distance the high speed electrons coming from the cathode can travel before losing so much energy that they have not enough left to ionize or produce luminosity. The field strength in the negative glow is exceedingly small, and this would imply from Poisson's equation ($\frac{dX}{dx}=4\pi\rho$) that the space charge density nearly vanishes. This must mean that the density of the electrons and positive ions is nearly equal. The existence of recombination in the negative glow is still a matter of discussion. Normally the light of the negative glow is caused by excitation of the air molecules. As the electrons reach the cathode edge of the negative glow they begin to lose energy by atomic or molecular collisions, and they eventually reach a velocity at which they can cause excitation. Thus, the electrons begin to become very numerous because of the cumulative ionization and not only have smaller energies, but the electrons produced by ionization also travel shorter distances before ionization energy is reached than the original secondary electrons. Thus, they ionize and excite very effectively. Visually, it would appear as if there were a marked increase in the intensity of the light in a very short distance. Actually, the negative glow is much more diffusely defined as would be expected from the rather large range of electron energies. Therefore, the negative glow may be regarded as the seat of ionization, the supply of positive ions preventing the electrons from building up a negative space charge.

The Faraday dark space is the part of the discharge lying between the negative glow and the positive column, the end of the dark space joining the negative glow is not sharply defined, and is due to the electron spread of energies. The density of the electrons in the dark space far exceeds the positive ion density as the electrons must travel the length of the dark space to gain enough energy from the field before they are capable of producing ionization. Recombination is also small because of the paucity of ions. The thickness of the Faraday dark space is inversely proportional to the current density and directly proportional to the pressure of the gas.

Thus, the electric field increases toward the anode until it reaches a point where it is intense enough to cause just enough ionization to compensate for the loss of positive ions by recombination and diffusion to the walls of the tube. From this point on to the anode is the positive column. This column, often called the "plasma", a word coined by Langmuir, usually exhibits striations[1] in air and impure gases. The pure gases will also exhibit striations if there are metastable atoms present.

---

1. The alternate light and dark spaces as evidenced in the photographs on page 3.

POTENTIAL DISTRIBUTION

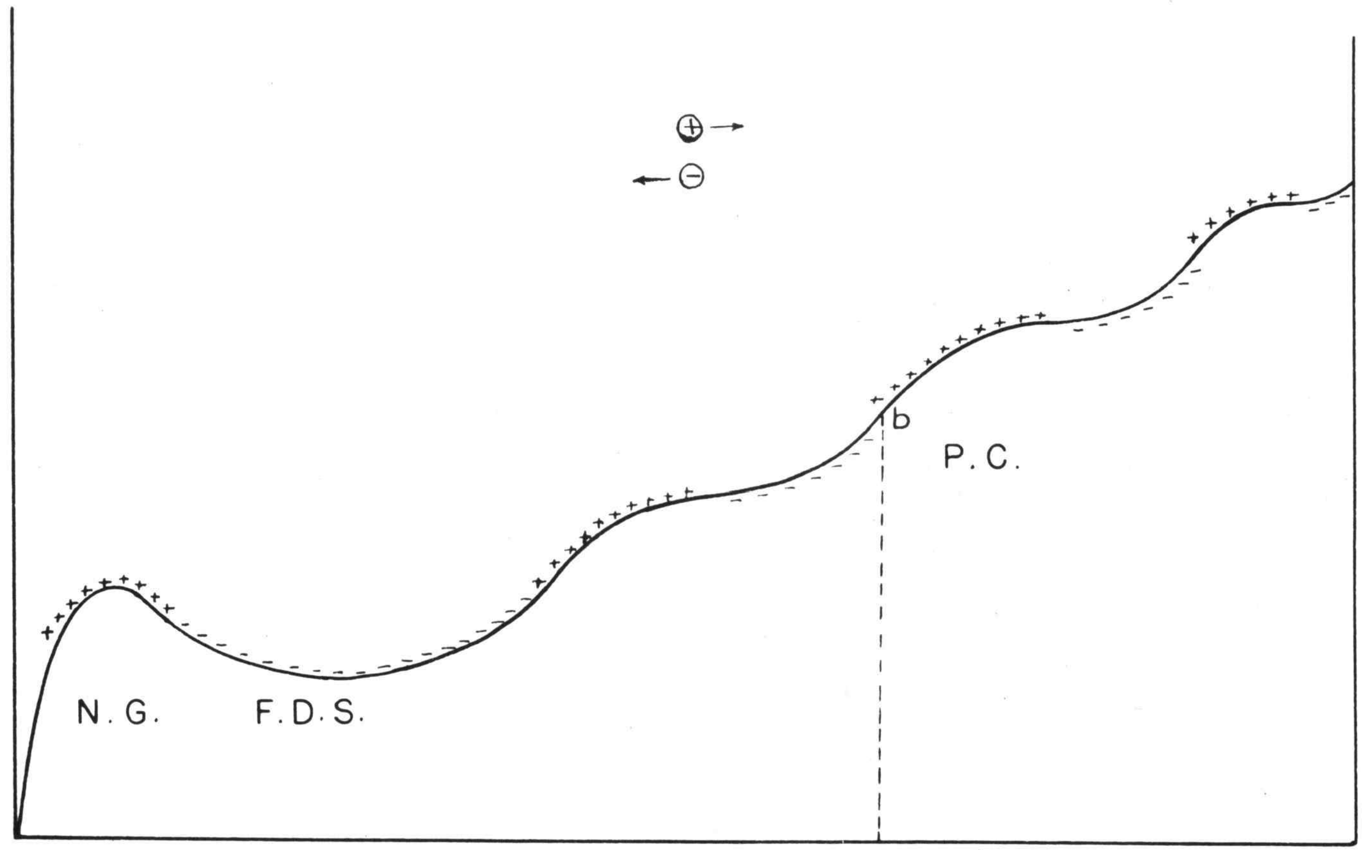

FIGURE I

Suppose, now, that an electron collides inelastically with a molecule at some point b. (3, p. 603) The electron mobility is least just before it is fast enough to make an inelastic collision. The negative space charge caused by the electrons varies inversely as the mobility of the electrons. This means that as soon as the electron has made an inelastic collision, there is an abrupt decrease in the negative space-charge. As the electron again gains speed the mobility decreases, the space-charge increases, and the process is repeated at another inelastic impact nearer the anode. Since the positive column is essentially a region of zero space-charge, these variations produced by successive inelastic impacts must give rise to alternate regions of positive and negative space-charge as indicated by the curve in Figure 1.

These variations in electric intensity increase the probability that other electrons will collide inelastically in the same regions because of the increased electric field strength in the region of an inelastic impact. The electrons moving in a field through the gas suffer elastic impacts below certain speeds and inelastic above them. This leads to the conclusion that there are successive regions in which the inelastic impacts will be concentrated. These regions of inelastic impact are characterized then by a positive space-charge, and they will be separated by regions of negative space charge and sufficient potential drop to allow the electrons to gain sufficient speed to cause more inelastic impacts. Inelastic impacts result in ionization or excitation of the molecules; therefore, these regions will have maximum luminosity.

From consideration of the fundamental properties of electrons, ions and molecules, we can infer the potential distribution as indicated in Figure 1.

In order to study experimentally the potential distribution and ion concentration in the discharge, the method of Langmuir, (6, p. 731) which consists of an exploring electrode, is employed.

Consider a plane square probe-electrode, P, which is placed parallel to the axis of the tube. (8, p. 237) Let V_x indicate the potential of the plasma at the position of the probe. Then $V = V_x - V_p$ may be made negative or positive as is desired. First, let us consider V strongly negative so that even the highest energy electrons are repelled by the probe. The positive-ion densities in the plasma are of the order of 10^8 ions/cm^3 or greater and thus with V negative there will be a positive space-charge limited current to the probe. This will cause a positive ion space-charge sheath to form around the probe and will appear visually as a dark space representing a region of no recombination of the positive ions or excitation of the molecules. The actual target area for the positive ions is the outer surface area F of the ion sheath. The probe current, i_p, then will equal the positive ion current, i_f, to the area F, provided there is no ionization, recombination or electron emission from the probe within the positive ion sheath.

The positive ions diffuse into the sheath giving a probe current $i_+ = \frac{FeN_+\bar{c}_+}{4}$ where $\frac{N_+\bar{c}_+}{4}$ is the number of ions of average velocity $\bar{c}$ striking unit area per second from a space containing N_+ ions per cubic centimeter. This space-charge-limited current can also be represented by an equation deduced by Child (1, p. 492) in 1911.

$$J_+ = \frac{i_+}{F} = \frac{1}{9\pi}\sqrt{\frac{2e}{m}}\,\frac{V^{3/2}}{d^2}$$

where d = sheath thickness and m = mass of a positive ion.

V does not alter the plasma outside the sheath, and thus F, N_+ , and $\bar{c}$ are constant; consequently, j_+ also is constant for strongly negative values of V. By measuring j_+ and d the potential V can be obtained.

When the value of V_p becomes sufficiently less negative to V_x, the faster electrons can penetrate the sheath and reach the probe. Since $i_p = i_+ - i_-$, the probe current will decrease with the increasing negative electron current i_- . i_- may be determined from i_p and the measured values of i_+ at high negative probe potential. The magnitude of i_- can also be calculated from the Maxwellian distribution equation.

$$N = \frac{N_-}{\alpha\sqrt{\pi}} e^{-\frac{c_x^2}{\alpha^2}} dc_x$$

This means that out of N_ electrons per cubic centimeter in the plasma, N_x of them will have velocity components normal to the probe between c_x and $c_x + dc_x$. $\frac{AN_x c_x}{4}$ will be the number striking the probe per second. Thus,

$$i_- = \frac{AeN_x c_x}{4} = \frac{AeN_-}{4\sqrt{\pi}} \int_{c_x}^{\infty} \frac{c_x}{\alpha} e^{-\frac{c_x^2}{\alpha^2}} dc_x = \frac{AeN_-\alpha}{4} e^{-\frac{c_x^2}{\alpha^2}}$$

where
$$\alpha^2 = \frac{2kT_-}{m_-}$$

T_ is the electron temperature in degrees Kelvin and m_ is the electron mass, and

$$Ve = \tfrac{1}{2} m c_x^2$$

therefore:

$$J_- = \frac{i_-}{A} = \frac{AeN_-}{A} \sqrt{\frac{kT_-}{2\pi m_-}} e^{-\frac{Ve}{kT_-}}$$

$$\ln J_- = \ln\left(\frac{eN_-}{\sqrt{2}} \sqrt{\frac{kT_-}{\pi m_-}}\right) - \left(\frac{Ve}{kT_-}\right)$$

$$\ln J_- = B - \frac{Ve}{kT_-}$$

where B = constant.

The log $j_- - V$ curve is linear, the slope being given by

$$\frac{d(\ln j_-)}{dV} = -\frac{e}{kT_-} = -\frac{1.17 \times 10^4}{T_-}$$

This relation allows the evaluation of the electron temperature T_. This linear curve seems to bear out the assumption of a Maxwellian distribution of velocities. If we designate as ΔV_p , the difference in potential for two values of Vp, Vp_1 and Vp_2 at which j_{-1} and j_{-2} are in the ratio of 1 : 2.718, then

$$T_- = 1.17 \times 10^4 \Delta V_p$$

This procedure for determining the electron temperature is the first step in the evaluation of the remaining plasma variables.

Further decrease of the negative probe potential leads to a value of $V = V_{i_p=0}$ such that the probe current $i_p = 0$ and thus $i_+ = i_-$. This is the point where the electron current due to diffusion equals the positive ion space-charge-limited current. At $V = V_{i_p=0}$

$$i_+ = \frac{eN_+\bar{C}_+}{4} = \frac{eN_-\bar{C}_-}{4} e^{-\frac{V_{i_p=0}e}{kT_-}} = i_-$$

Assuming now that $N_- = N_+$ as is usually the case in undisturbed plasma, we can write

$$V_{i_p=0} = \frac{kT_-}{e} \ln \frac{\bar{c}_-}{\bar{c}_+}$$

$$V_{i_p=0} = \frac{kT_-}{e} \ln \frac{T_- M_+}{T_+ M_-}$$

$V_{i_p=0}$ is also called the wall potential. As the negative potential is reduced further, a point will be reached for which $V=0$. This means that the probe will be at the plasma potential, and both the electrons and positive ions reach the probe in proportion to their normal rates of diffusion. Since $V=0$

$$e^{-\frac{Ve}{kT_-}} = e^0 = 1$$

then at V_x

$$J_{-V_x} = eN_- \sqrt{\frac{kT_-}{2\pi m_-}}$$

The positive ion current drops to zero very rapidly with a low value of positive V, thus the log $J_- - V$ curve undergoes a sudden change of slope. This fixes the values of V_x for which $V = 0$ and may be obtained easily from the log $J_- - V$ curve at the discontinuity.

Also $$J_{+V_x} = \frac{N_x \bar{c}_x e}{4} = eN_+ \sqrt{\frac{kT_+}{2\pi m_+}}$$

because $$C_x = \sqrt{\frac{8kT_+}{\pi m_+}}$$

Summing up, we can evaluate by our one series of probe measurements:

(1) The electron temperature from the slope of the $\log j - V$ curve.

(2) The electron current density j_- from i_p at $V = 0$, $V_p = V_x$ or $i_p = i_- - i_+$ and knowing A. It must be remembered that at $V = 0$ the probe area is A and not F since the sheath is not present.

(3) The electron density n_- from j_- and T_- at $V = 0$.

(4) The temperature of the positive ions, from j_+ at $V = 0$ assuming a normal discharge where $N_- = N_+$.

If the probe becomes even more positive, there will be a space-charge limited electron current; positive ion current, therefore, being zero.

A great deal can thus be learned from exploring electrode measurements providing the basic assumptions and Maxwell's law hold. If Maxwell's law does not hold, as would be indicated by non-linearity of the $\log j - V$ curves, one could attempt further work using the distribution due to Druyvesteyn. (4, p. 790)

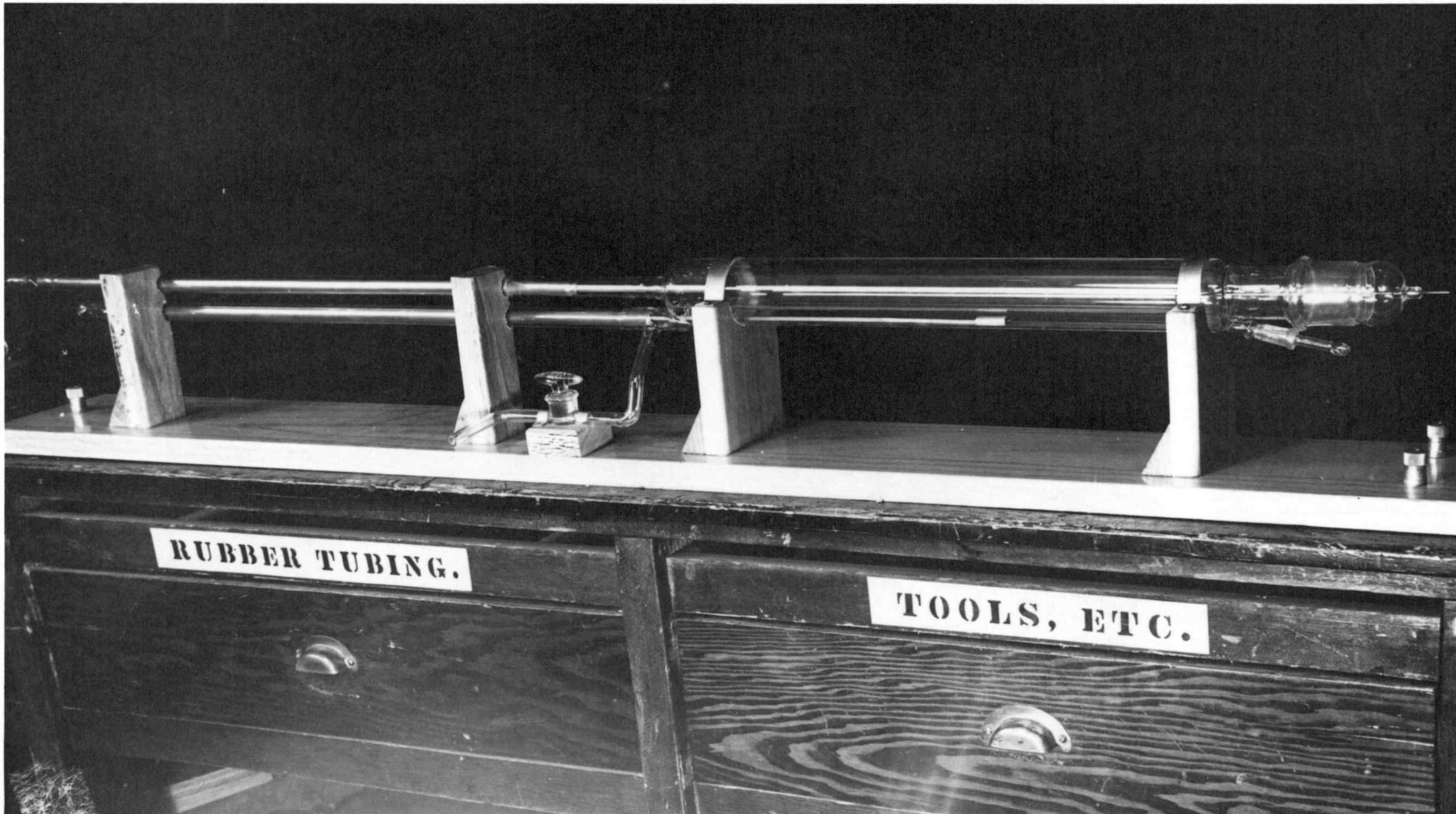
RUBBER TUBING.
TOOLS, ETC.

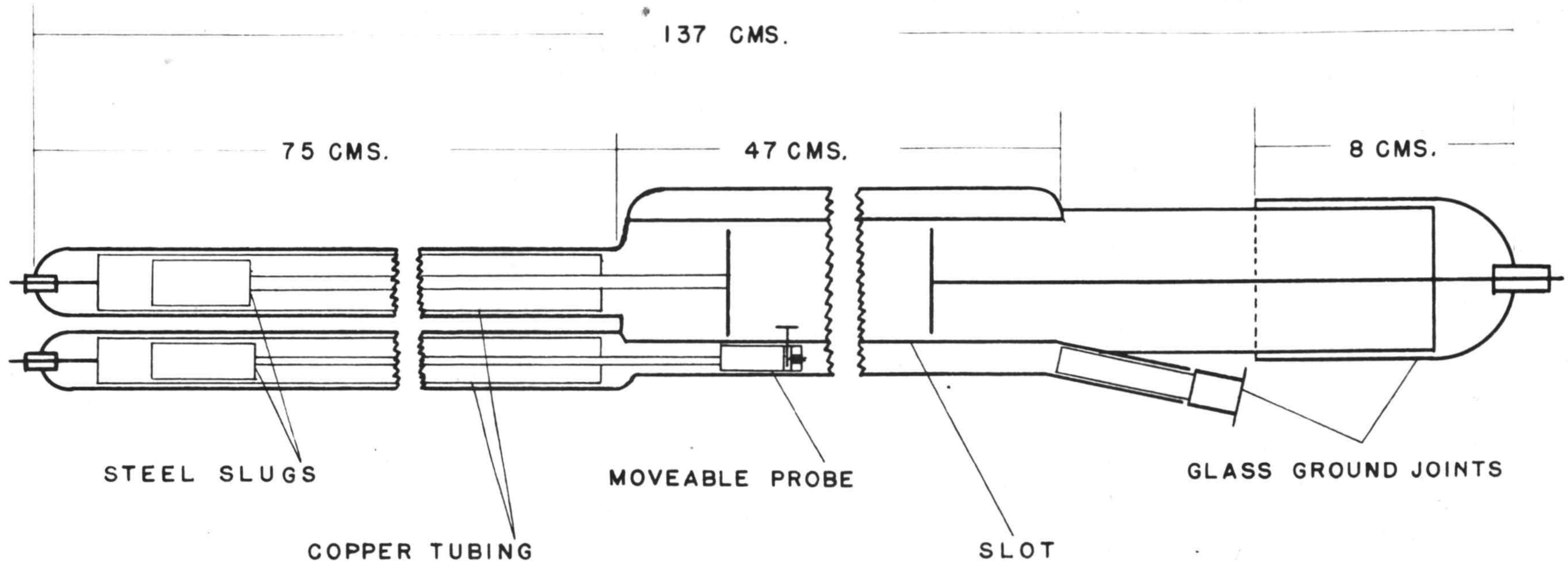

GAS DISCHARGE TUBE

FIGURE 2

Construction

In order to be able to make a plot of the plasma potential versus distance from cathode, it is necessary to have a probe capable of making continuous probe measurements for the entire length of the discharge. To accomplish this it is necessary to provide access for the probe to the plasma of the discharge.

The method used provides access by a long narrow slot through which the probe protrudes into the plasma. The slot should be narrow enough so as to cause no appreciable effect upon the plasma.

Attempts to slot the pyrex tube were first made using two diamond-impregnated steel saws of different widths. Precautions to prevent excessive vibrations in the sawing process, such as filling the tube with wax and surrounding the outside with plaster of paris, were found to be necessary. The saw first made its cut through the plaster of paris and then into the pyrex. The area being sawed through was sprayed with a direct stream of water to act as a lubricant and also to help dissipate the heat. The cutting speed of about 400 rev min^{-1} was maintained by a shunt wound d.c. motor geared down by a system of belt pulleys. Higher speeds seemed to cause excessive chipping of the edges. The edges of the slot were still badly chipped, however, even with these precautions. It was decided that the cause was the hard bond holding the diamond dust in place.

The next and only successful attempt employed the above mentioned precautions but a commercial grinding wheel of carborundum set in a soft rubber bond was used in place of the diamond saw. After the plaster of paris had been cut through and the cut into the glass started, it was found that precaution should be used at this time to lower the stock slowly onto the wheel. Lowering rapidly will bow the thin blade causing it to cut a slot much wider than the width of the blade. The stock was fed as slowly as possible into the wheel in such a direction as to be opposite to the rotational direction of the grinding wheel. This grinding process produced bad strains along the edges of the slot which could be observed by means of two polaroid discs. It is important to anneal the ends of the slot to prevent cracking, which occurs during the heating necessary to form the ring seals.

The distance between the cathode and anode was made variable by having the cathode movable by means of a magnet outside the evacuated region. As can be seen in Figure 2 the upper extension of the main tube contains a 1/2 in. hollow copper tube inside of which is a 2 in. mild steel slug with a .005 in. clearance. To the slug is attached a

3/16 in. hollow brass tube of sufficient length to protrude past the glass ground joint when the slug is at the maximum position. In this way the electrodes may be changed so that different materials can be studied. Electrical contact is made from the brass tube to the aluminum bearing, which is attached to the copper tube. A .040 nickel lead is soldered to the copper tube and then passed out through the tube by a uranium glass to tungsten seal.

The probe is caused to move in the same manner as the movable cathode; a square solid brass rod being used in place of the round one used for the cathode. A rectangular slug of brass terminating the rod is pierced with a 1/16 in. hole. Different probes may be substituted by dropping them down through the slit into the hole and are held in place by a set screw which may be tightened by an allen wrench inserted through the small glass ground joint.

CIRCUIT DIAGRAM

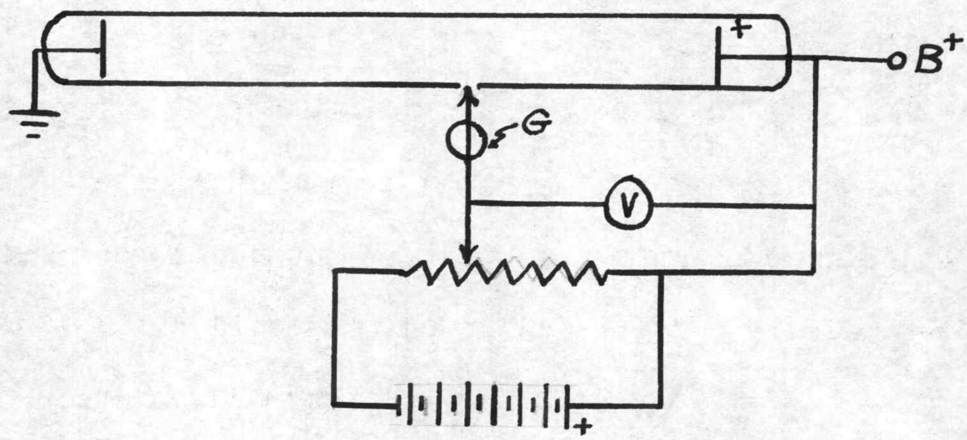

The galvanometer used in the above circuit was accurate to .5 percent with an internal resistance of 198 Ω. A Simpson meter was used for the voltmeter with an internal resistance of 20,000 Ω per volt. With the rheostat in its maximum position, the error made by neglecting the voltage drop across the 100,000 Ω resistance is only one part in 200. The error is negligible at voltage readings of 150 volts and below. The power supply had a one volt ripple at 1,500 volts. The voltmeter as shown reads directly $V_p - V_a$ where V_p is the probe potential and V_a is the anode potential.

EXPERIMENTAL RESULTS

A series of measurements was made for four different probe locations. The consistency of this data is evident from the similarity of Figures 3 - 8, pp. 26, 28, 30, 32, 34, 36. Calculations have been made using the data tabulated on Table 5, p. 33, and plotted in Figure 7, p. 34.

Referring to Figure 7, the dashed straight line indicates the theoretical positive ion current that would exist if there were no electrons being collected by the probe. Thus, the electron current may be found from $i_{-} = i_p - i_{+}$ by extrapolation. Figure 8, p. 36, shows a plot of the logarithm of this calculated electron current versus $V_p - V_a$. The linearity of the bottom portion of the curve seems to indicate the correctness of the assumption of a Maxwellian distribution of velocities in the positive striated column.

The space potential may be estimated from Figure 8 by the intersection of the two straight lines $\overline{MN}$ and $\overline{NO}$.

This log j_{-} - V curve should have a sharp discontinuity at V_x instead of the smooth curve evident. This makes the choice of V_x difficult. This break point is not sharp due, probably, to such effects as electron emission from the probe surface, ionization by electrons in the area near the probe, and electron reflection from the probe.

The calculations below give the possible information available from the one series of probe measurements:

1. Electron Temperature

From Figure 8, ΔV_p = 6.6 volts when i_- and i_{-2} are in the ratio of 1:2.718. Thus

$$T_- = 1.17 \times 10^4 \times \Delta V_p \ {}^\circ K$$

$$T_- = 1.17 \times 10^4 \times 6.6 \ {}^\circ K = 7.7 \times 10^4 \ {}^\circ K$$

2. Electron Current Density at V_x

Area of the probe A = .095 square centimeters.

$$\text{Log } i_{-V_x} = 3.85 \quad \text{(from figure 8)}$$

$$i_- = 47.6 \times 10^{-6} \text{ amperes}$$

$$J_{-V_x} = \frac{47.0 \times 10^{-6}}{.095} \frac{\text{amperes}}{\text{cm}^2} = 4.95 \times 10^{-4} \frac{\text{amperes}}{\text{cm}^2}$$

3. Electron Density

$$J_{-V_x} = eN_- \sqrt{\frac{kT_-}{2\pi m_-}}$$

$$N_- = \frac{4.95 \times 10^{-4} \times 3 \times 10^{10}}{4.80 \times 10^{-10}} \sqrt{\frac{2\pi \times 9 \times 10^{-28}}{1.3 \times 10^{-16} \times 7.7 \times 10^4}} \Big/ \text{cm}^3$$

$$N_- = 7.2 \times 10^8 / \text{cm}^3$$

4. The Positive Ion Temperature

$$J_{+v_x} = \frac{i_{+v_x}}{A} = \frac{0.1 \times 10^{-6}}{0.095} \frac{\text{amperes}}{\text{cm}^2} = 1.05 \times 10^{-6} \frac{\text{amperes}}{\text{cm}^2}$$

$$m_+ = 26.6 \times 10^{-24} \text{ grams}$$

$$N_- = N_+ = 7.2 \times 10^{8}/\text{cm}^3$$

$$T_+ = \frac{2\pi m_+}{k} \left(\frac{J_{+v_x}}{e N_+} \right)^2$$

$$T_+ = 9900^\circ K$$

Thus with the satisfying results obtained for the electron and positive ion temperatures, even though the surface had not been outgassed, the apparatus will serve well for student use in the laboratory.

DATA SHEET NO. 1

Probe Position - 3.1 centimeters
Pressure - 2 millimeters
Anode Potential - 1.0 kv
Plate Current - 1.3 ma

$V_p - V_a$	I_p	$V_p - V_a$	I_p
400	8.60	160	1.30
380	5.80	150	1.20
360	4.30	140	1.10
340	3.63	130	1.00
320	3.40	120	.85
300	2.90	110	.78
280	2.52	100	.62
250	2.35	95	.42
240	2.26	90	.10
230	2.20	85	- 1.60
220	2.08	80	- 4.1
210	1.87	75	- 7.3
200	1.76	70	-12.4
190	1.60	65	-19.4
180	1.50	62.5	-23.5
170	1.40		

Table 1

Fig. 3

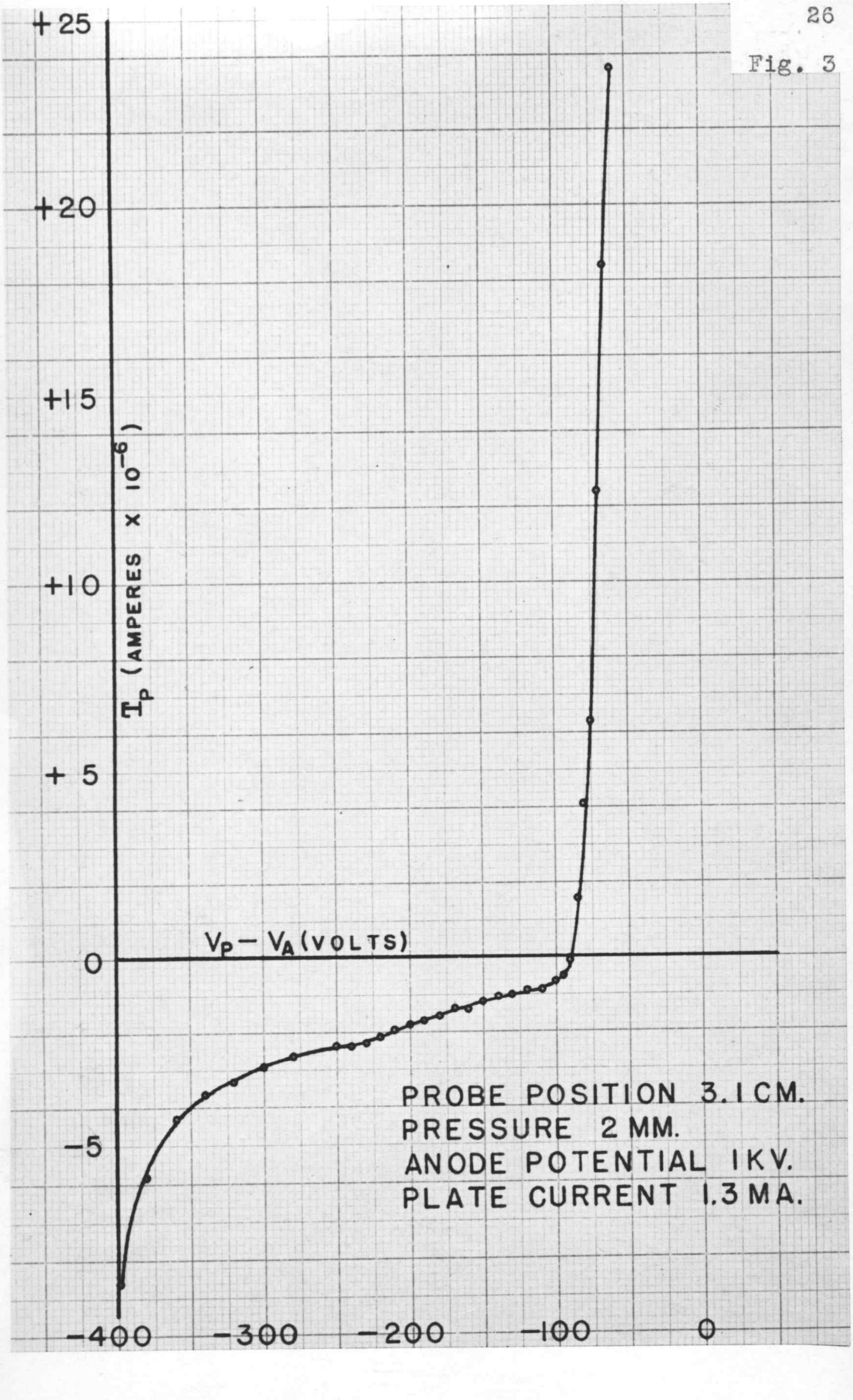
+25
+20
+15
+10
+ 5
0
-5
I_p (AMPERES x 10^{-6})
$V_P - V_A$ (VOLTS)
-400
-300
-200
-100
0
PROBE POSITION 3.1 CM.
PRESSURE 2 MM.
ANODE POTENTIAL 1 KV.
PLATE CURRENT 1.3 MA.

D A T A   S H E E T   N O. 2

Probe Position - 3.1 centimeters
Pressure - 500 microns
Anode Potential - 1.1 kv
Plate Current - .67 ma

$V_p - V_a$	I_p	$V_p - V_a$	I_p
390	14.6	145	1.00
380	11.0	140	1.00
360	7.0	135	1.00
340	5.2	130	.90
320	4.1	125	.85
300	3.5	120	.80
280	2.9	115	.70
260	2.5	110	.70
240	2.27	105	.60
210	1.95	100	.60
200	1.90	95	.50
195	1.83	90	.40
190	1.80	85	.35
185	1.70	80	.20
180	1.50	75	- .80
175	1.40	70	- 2.0
170	1.35	65	- 3.6
165	1.20	60	- 6.8
160	1.20	55	-11.8
155	1.20	50	-18.2
150	1.10		

Table 2

Fig. 4

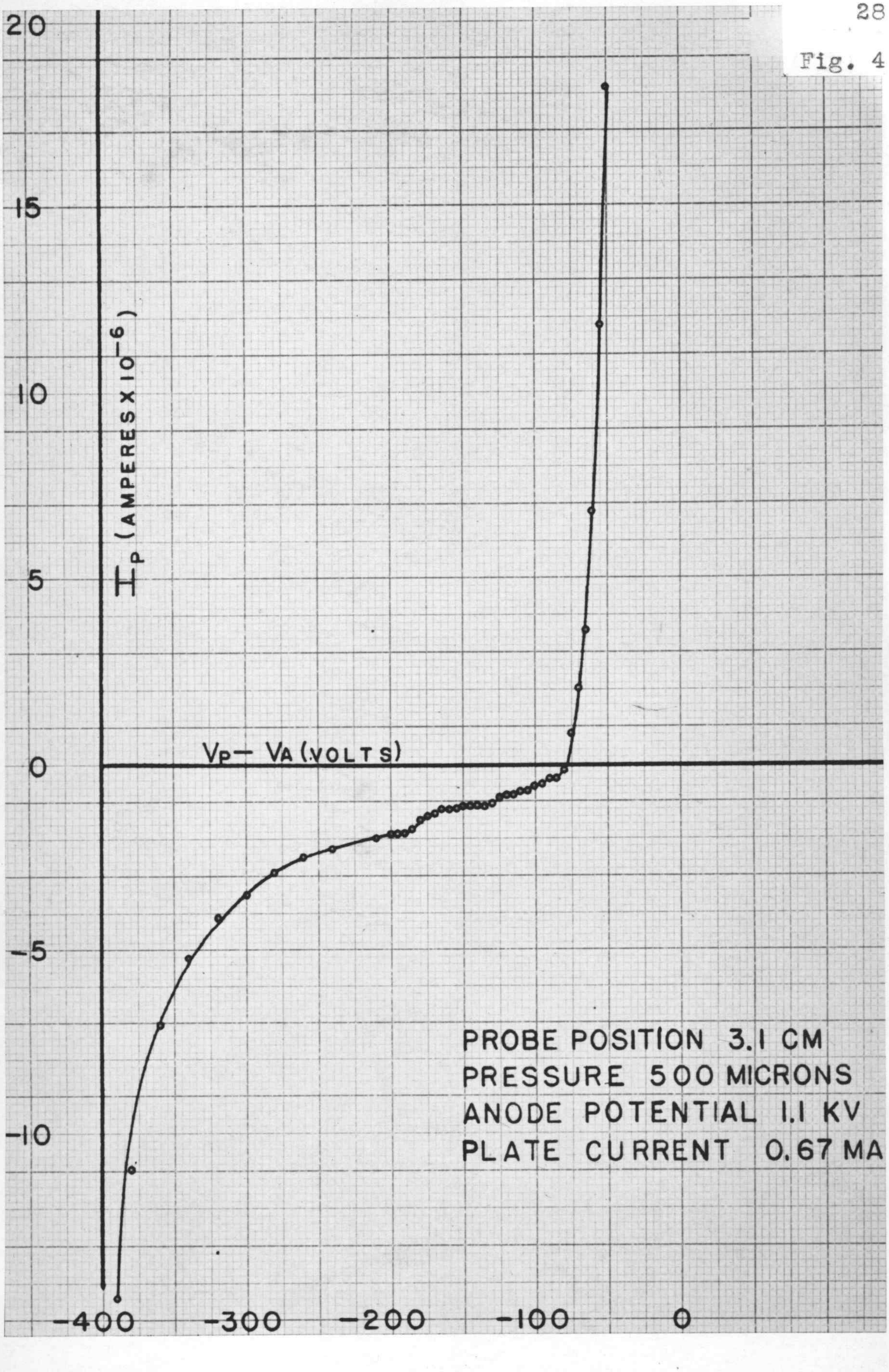
20
15
10
5
0
-5
-10
I_P (AMPERES X 10^{-6})
$V_P - V_A$ (VOLTS)
-400
-300
-200
-100
0
PROBE POSITION 3.1 CM
PRESSURE 500 MICRONS
ANODE POTENTIAL 1.1 KV
PLATE CURRENT 0.67 MA

DATA SHEET NO. 3

Probe Position - 5.0 centimeters
Pressure - 500 microns
Anode Potential - 1.1 kv
Plate Current - 0.67 ma

$V_p - V_a$	I_p	$V_p - V_a$	I_p
390	7.2	150	.80
380	5.9	145	.80
360	4.4	140	.70
340	3.6	135	.70
320	3.0	130	.60
300	2.5	125	.55
280	2.1	120	.50
260	1.9	115	.50
240	1.7	110	.40
220	1.4	105	.30
200	1.2	100	- .40
180	1.0	95	-1.50
175	.94	90	-3.00
170	.90	85	-5.20
165	.90	80	-9.50
160	.90	75	-14.2
155	.85	70	-25.

Table 3

Fig. 5

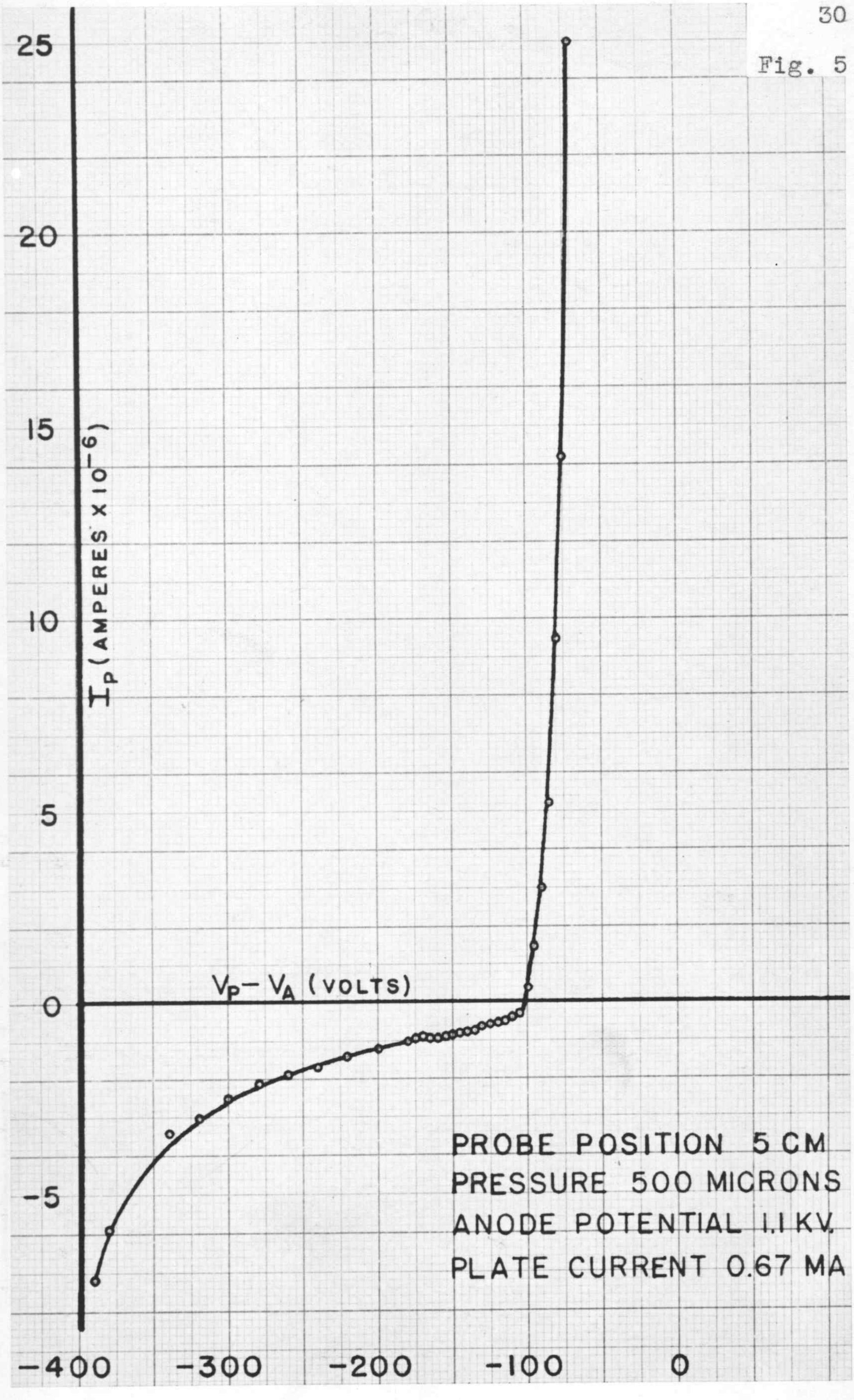

25
20
15
10
5
0
-5
I_P (AMPERES X 10^{-6})
$V_P - V_A$ (VOLTS)
-400
-300
-200
-100
0
PROBE POSITION 5 CM
PRESSURE 500 MICRONS
ANODE POTENTIAL 1.1 KV.
PLATE CURRENT 0.67 MA

DATA SHEET NO. 4

Probe Position - 7 centimeters
Pressure - 500 microns
Anode Potential - 1.1 kv
Plate Current - .67 ma

$V_p - V_a$	I_p	$V_p - V_a$	I_p
440	12.6	190	.95
420	7.7	180	.87
400	5.6	170	.75
380	4.4	160	.65
360	3.6	150	.60
340	3.0	140	.40
320	2.5	135	.30
300	2.2	130	- .30
280	1.9	125	- .75
260	1.6	120	- 3.70
240	1.4	115	- 6.30
220	1.2	110	-10.80
200	1.0	105	-18.3

Table 4

Fig. 6

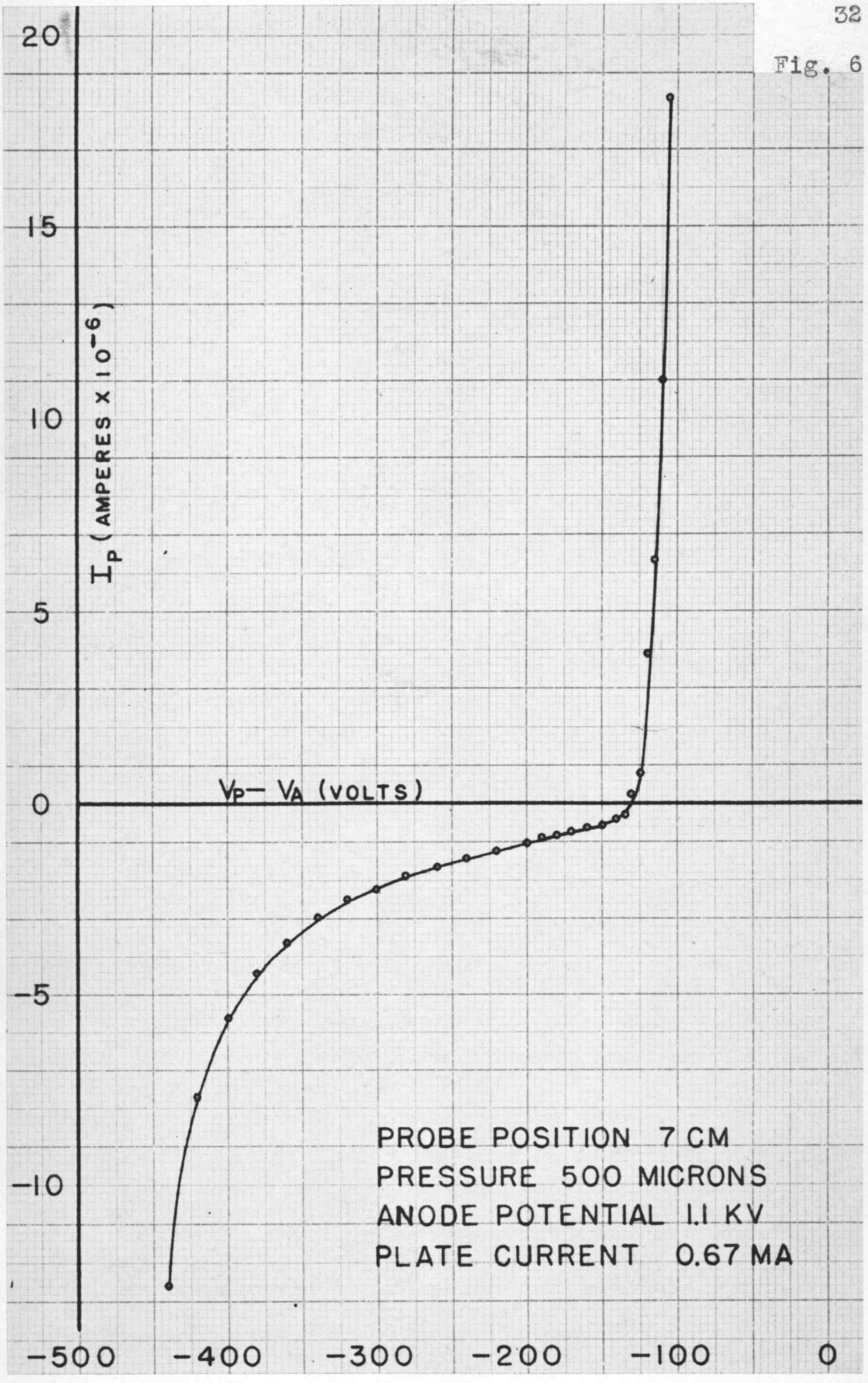
20
15
10
5
0
-5
-10
I_P (AMPERES x 10^{-6})
$V_P - V_A$ (VOLTS)
-500
-400
-300
-200
-100
0
PROBE POSITION 7 CM
PRESSURE 500 MICRONS
ANODE POTENTIAL 1.1 KV
PLATE CURRENT 0.67 MA

D A T A   S H E E T   N O.   5

Probe Position - 15 centimeters
Pressure - 300 microns
Anode Potential - 1.3 kv
Plate Current - 0.42 ma

$V_p - V_a$	I_p	$V_p - V_a$	I_p
400	-10.70	145	-1.85
380	- 9.80	140	-1.70
360	- 8.90	135	-1.40
340	- 8.10	130	-1.00
320	- 7.50	125	.20
300	- 6.40	120	1.40
280	- 5.75	115	3.37
260	- 5.10	110	6.20
240	- 4.50	105	11.40
220	- 3.90	100	21.60
200	- 3.40	95	31.0
180	- 2.80	90	44.5
170	- 2.70	85	57
165	- 2.60	80	70
160	- 2.50	77.5	78
155	- 2.24	75.0	82
150	- 2.10	70.0	85

Table 5

Fig. 7

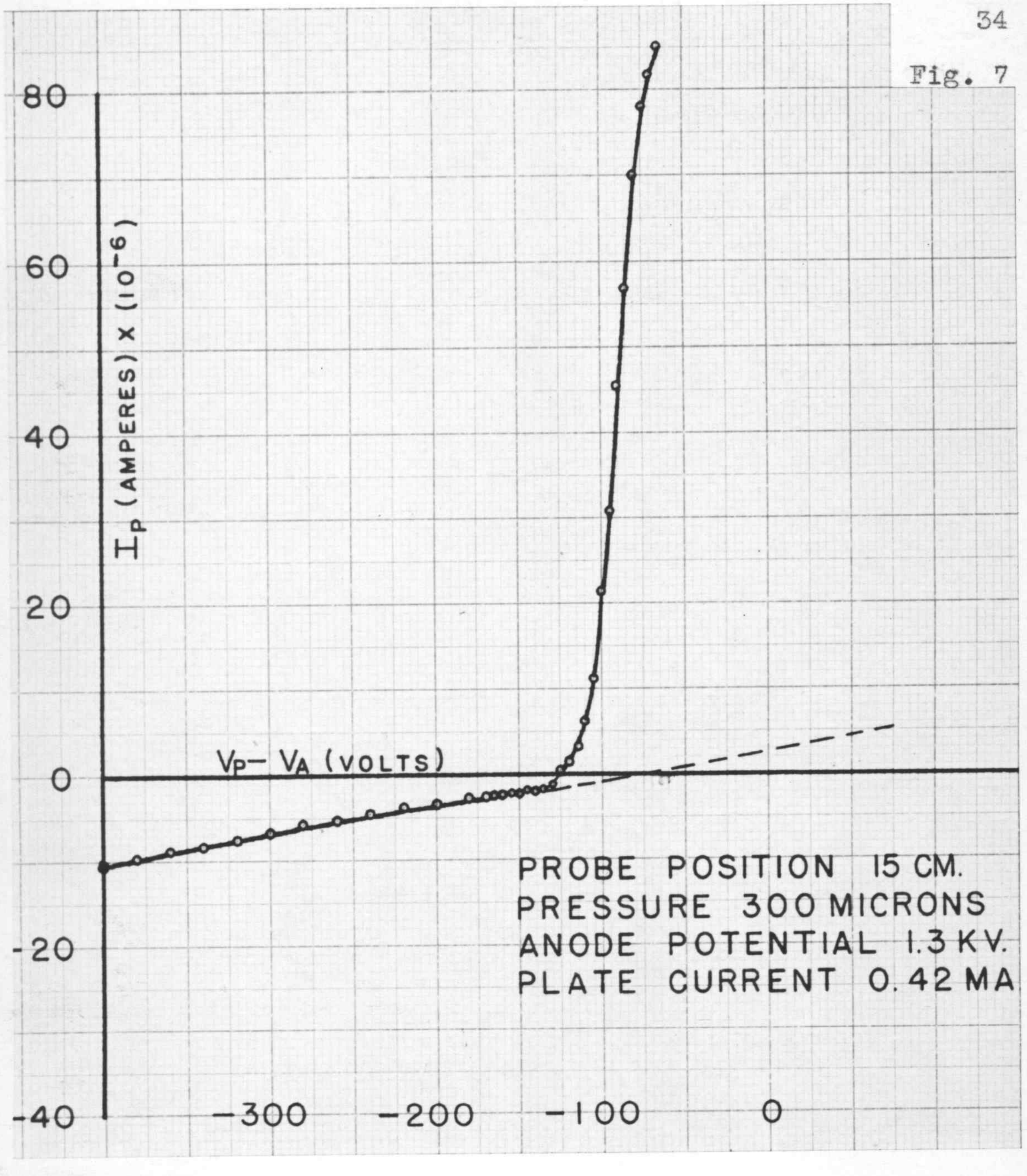
80
60
40
20
0
-20
-40
I_P (AMPERES) x (10^-6)
V_P - V_A (VOLTS)
-300
-200
-100
0
PROBE POSITION 15 CM.
PRESSURE 300 MICRONS
ANODE POTENTIAL 1.3 KV.
PLATE CURRENT 0.42 MA

D A T A   S H E E T   N O. 6

Probe Position - 15 centimeters
Pressure - 300 microns
Anode Potential - 1.3 kv
Plate Current - 0.42 ma

$V_p - V_a$	I_p	I_+	$I_- = I_p - I_+$	Log I_-
125	0.20	-1.10	1.30	0.26
120	1.40	- .97	2.37	0.86
115	3.37	- .83	4.20	1.44
110	6.20	- .69	6.89	1.93
105	11.40	- .55	11.95	2.48
100	21.60	- .41	22.01	3.09
95	31.0	- .27	31.27	3.44
90	44.5	- .13	44.63	3.80
85	57.0	.01	56.99	4.04
80	70.0	.15	69.85	4.25
77.5	78.0	.29	77.71	4.35
75.0	82.0	.43	81.57	4.40
70.0	85.0	.57	84.43	4.44

Table 6

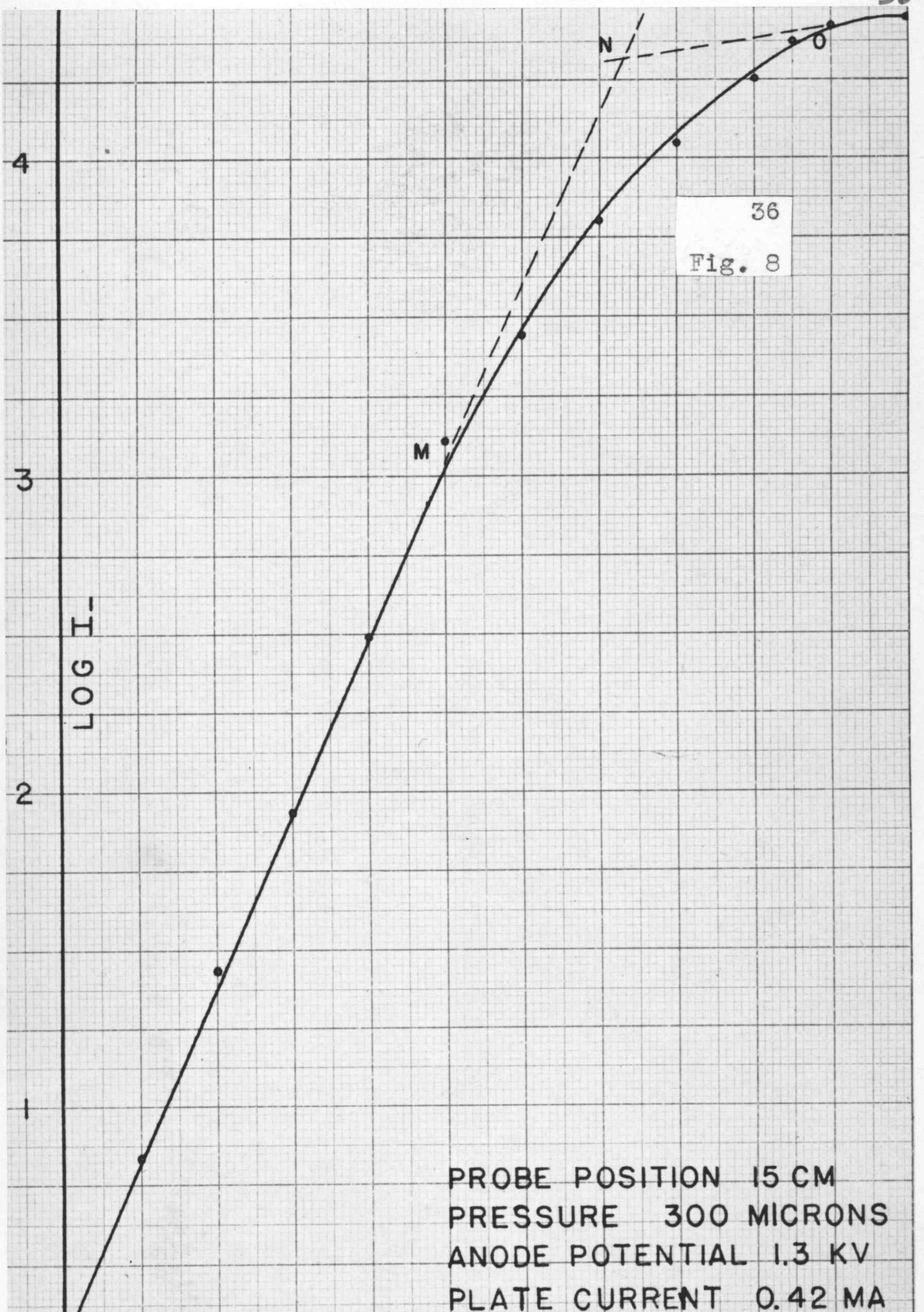
N
O
4
36
M
3
LOG I-
2
1
PROBE POSITION 15 CM
PRESSURE 300 MICRONS
ANODE POTENTIAL 1.3 KV
PLATE CURRENT 0.42 MA
$V_P - V_A$ (VOLTS)
-125
-100
-75

Fig. 8

LITERATURE CITED

1. Child, C. D. Discharge from hot cao. Physical review 32:492. 1911.

2. Compton, K. T. On the motions of electrons in gases. Physical review 22:333. 1923.

3. Compton, K. T., L. A. Turner and W. H. McCurdy. Theory of experiments relating to the striated glow discharge in mercury vapor. Physical review 24:597-603. 1924.

4. Druyvesteyn, M. J. Der Niedervoltbogen. Zeitschrift fur Physik 64:790. 1930.

5. Guntherschulze, A. and F. Keller. Die Anregung von Spektrallinien durch den Stoss longsamen positiver Ionen. Zeitschrift fur Physik 72:143. 1931.

6. Langmuir, I. Positive ion currents in the positive column of the mercury arc. General electric review 26:731. 1923.

7. Langmuir, I. and H. Mott-Smith. Studies of electric discharges in gases at low pressures. General electric review 27:449, 538, 616, 762, 810. 1924.

8. Loeb, Leonard. Fundamental processes of electrical discharges in gases. New York, John Wiley & Sons, Inc., 1947. 717p.

9. Thomson, J. J. Conduction of electricity through gases. 3d ed. London, Cambridge University Press, 1933. 608p.